

# Capacity Analysis of One-Bit Quantized MIMO Systems with Transmitter Channel State Information

Jianhua Mo, *Student Member, IEEE*, and Robert W. Heath, Jr., *Fellow, IEEE*

**Abstract**—With bandwidths on the order of a gigahertz in emerging wireless systems, high-resolution analog-to-digital converters (ADCs) become a power consumption bottleneck. One solution is to employ low resolution one-bit ADCs. In this paper, we analyze the flat fading multiple-input multiple-output (MIMO) channel with one-bit ADCs. Channel state information is assumed to be known at both the transmitter and receiver. For the multiple-input single-output channel, we derive the exact channel capacity. For the single-input multiple-output and MIMO channel, we derive bounds on the high signal-to-noise ratio (SNR) capacity. Two efficient methods are proposed to design the input symbols to approach the capacity achieving solution. We incorporate millimeter wave channel characteristics and find the bounds on the high SNR capacity. The results show how the number of paths, number of transmit antennas, and number of receive antennas impact the capacity at high SNR. In the special case when there is only one path, we find the capacity-achieving transmission strategy. Our results provide insights into the high SNR behavior of the MIMO capacity with one-bit ADCs.

**Index Terms**—Analog-to-digital convertor, one-bit quantization, MIMO channel, millimeter Wave, stochastic resonance

## I. INTRODUCTION

Bandwidth and antennas are growing in next generation wireless systems. A main reason is due to the use of millimeter wave (mmWave) carrier frequencies in personal area networks [2], local area networks [3], and likely even cellular networks [4]. The channel bandwidths in mmWave systems are larger than those used in lower frequency UHF (ultra high frequency) systems. For example, in IEEE 802.11ad the bandwidth is 2.16 GHz while in potential mmWave cellular applications, bandwidths of 500 MHz or more are being considered [5]. Antenna arrays are important for mmWave systems. They provide array gain that helps mmWave systems achieve a favorable link margin. Due to the small carrier wavelength, a large number of co-located antennas can be deployed within a fixed antenna area in mmWave systems. For example, some 802.11ad chipsets use 32 antennas [6], while mmWave cellular applications envision hundreds of antennas at the base station and perhaps a dozen on the handset [5]. This motivates the study of MIMO systems with large numbers of antennas and higher channel bandwidths.

High bandwidth channels introduce new challenges in system design compared with design at lower frequencies [7]. One major issue is the power consumption associated with the

analog-to-digital conversion. In conventional multiple-input multiple-output (MIMO) receiver designs, the analog-to-digital converters (ADCs) are expected to have high resolution (e.g., more than 8 bits) and act as transparent waveform preservers. In channels with larger bandwidths, the corresponding sampling rate of the ADCs scales up. Unfortunately, high-speed (e.g., more than 1 GSample/s), high-resolution ADCs are costly and power-hungry for portable devices [8]–[10]. For example, in an ideal  $b$ -bit ADC with flash architecture, there are  $2^b - 1$  comparators and therefore the power consumption grows exponentially with the resolution [8]. At present, commercially available ADCs with high-speed and high-precision consume power on the order of several Watts [11]. Furthermore, because most communication systems exploit some form of MIMO operation, multiple ADCs will be needed to quantize the received signals from multiple antennas separately if conventional digital baseband processing of all antenna outputs is assumed. Therefore, the total power assumption can be excessive, especially at the mobile station.

The most direct solutions to the power assumption bottleneck are to reduce the sampling rate and/or the quantization resolution of ADCs. The sampling rate can be reduced by employing a special ADC structure called the time-interleaved ADC (TI-ADC) where a number of low-speed, high-precision ADCs operate in parallel. The main drawback of the TI-ADC is the mismatch among the sub-ADCs in gain, timing and voltage offset which can cause error floors in receiver performance (though it is possible to compensate the mismatch at the price of higher complexity of the receiver [12], [13]). An alternative to high resolution ADCs is to live with ultra low precision ADCs (1-3 bits), which reduces power consumption and cost.

In this paper, we consider MIMO systems in which a one-bit ADC is used for each inphase and quadrature baseband received signal. The main advantage of this architecture is that the ADCs can be implemented with very low power consumption [14]. The architecture also simplifies the overall complexity of the circuit, for example automatic gain control (AGC) may not be required [15]. Several aspects of one-bit ADCs have been investigated in prior work including capacity analysis of the single-input single-output (SISO) channel [16]–[19] and MIMO channel [20]–[25], channel estimation [26]–[30], synchronization [31] and receiver design [32]–[35]. In related previous work on MIMO channel capacity [20]–[25], the channel state information (CSI) is assumed unknown at the transmitter.

In this paper, we analyze the capacity of the one-bit quantized MIMO channel with both channel state information at the transmitter (CSIT) and channel state information at the

The authors are with Wireless Networking and Communications Group, The University of Texas at Austin, Austin, TX 78712, USA (Email: {jhmo, rhealth}@utexas.edu.)

The material in this paper was presented in part at the 2014 Information Theory and Applications Workshop [1].

This work is supported in part by the National Science Foundation under Grants No. 1218338 and 1319556.

receiver (CSIR). With one-bit quantization, the outputs of the ADCs are discrete and finite. As a result, the capacity is achieved by a discrete input distribution [17], [36]. This is in contrast with unquantized MIMO systems where the optimal input distribution is continuous. Although it is finite-dimensional, finding the optimal discrete input distribution is a challenging problem that depends on the CSIT and CSIR. In [17], the capacity of the real-valued SISO channel with CSIT and CSIR was considered. For one-bit quantization, binary antipodal signaling was found to be optimal. It was also shown that in the low SNR regime, the use of low-resolution ADCs incurs a surprisingly small loss in spectral efficiency compared to unquantized observations. In the block fading SISO channel without CSIT and CSIR, it was proven in [24] that the capacity is achieved by on-off QPSK signaling where the on-off probability depends on the coherence time. However, the results in [17] and [24] do not really extend to the MIMO channel.

The most related work to our contribution is [23] where the one-bit quantized MIMO channel with only CSIR was considered. It was found that under the constraint that each antenna transmits signals independently and with equal power, independent QPSK signaling across different antennas is optimal in the low SNR regime. In addition, there is a reduction of low SNR channel capacity by a factor  $2/\pi$  ( $-1.96$  dB) due to one bit quantization. The results, unfortunately do not apply to medium or high SNR regimes. Hence remains of interest to provide a complete characterization of the high SNR capacity in quantized MIMO systems.

In [20]–[22], the capacity of the quantized MIMO channel was derived under different assumptions. The input symbols, though, were only BPSK or QAM symbols since they all assumed there is no CSI at the transmitter. Therefore, what is called *capacity* in [20]–[22] is actually *the mutual information* or *an achievable rate* since the input distributions are not optimized. Though reasonable for practical implementation, without a carefully designed input distribution, the mutual information of quantized MIMO channel may achieve its maximum at a finite SNR (this phenomenon is called *stochastic resonance*). With CSIT, the transmitter can implement beamforming to obtain array gain and can also design the transmitted constellation to achieve higher achievable rates. Therefore, it is interesting to consider the quantized channel with both CSIT and CSIR.

In this paper, we evaluate the capacity of the general MIMO channel with one-bit quantization assuming both perfect CSIT and CSIR. Throughout the paper, we focus mostly on the capacity when the ADCs operate at high SNR, i.e., the signals at the inputs of the ADCs have high SNR. This implies that the noise will not likely result in a sign change of the received signals. The use of beamforming at the transmitter makes a high SNR assumption reasonable since the received SNR includes the transmit beamforming gain. Since there are only finite number of bits available at the output of the ADCs, the channel capacity is upper bounded at high SNR and thus the degrees of freedom is zero which is in striking contrast with unquantized MIMO systems. Our initial work [1] presented a loose bound on high SNR capacity of MIMO channel. In this

paper, we derive a tighter bound.

The main contributions of this paper are summarized as follows.

- We find the capacity of the multiple-input single-output (MISO) channel with one-bit quantization in the whole SNR regime.
- We derive the high SNR capacity of the single-input multiple-output (SIMO) channel with one-bit quantization. We also find a closed-form expression for the SIMO channel capacity when the receiver has a large number of antennas. We apply a numerical algorithm to obtain the capacity-achieving input distribution.
- We provide bounds on the high SNR capacity of the MIMO channel with one-bit quantization. The decoding process at the receiver is similar to finding the transmitted symbols satisfying a series of linear inequalities. Based on this observation, we develop accurate bounds on the high SNR capacity by relating it to a problem in classical combinatorial geometry. Two computationally efficient methods are proposed to design the input alphabet such that the high SNR capacity is achieved.
- We find the high SNR capacity of a sparse mmWave channel. We show that the high SNR capacity is mainly limited by the number of paths in the mmWave propagation environment. In a special case when there is only one single path, we propose a capacity-achieving transmission strategy.

The paper is organized as follows. In Section II, we describe a MIMO system with one-bit quantization. In Section III, we present capacity analysis of the one-bit quantized MIMO channel. Numerical methods to optimize the distribution of input symbols are shown in Section IV. We then consider the quantized mmWave MIMO channel in Section V. Simulation results are shown in Section VI, followed by the conclusions in Section VII.

*Notation* :  $a$  is a scalar,  $\mathbf{a}$  is a vector and  $\mathbf{A}$  is a matrix.  $\angle x$  represents the phase of a complex number  $x$ .  $\mathbf{x}_{i:j}$  is the vector consisting of  $\{x_k, i \leq k \leq j\}$ .  $\text{tr}(\mathbf{A})$ ,  $\mathbf{A}^T$  and  $\mathbf{A}^*$  represent the trace, transpose and conjugate transpose of a matrix  $\mathbf{A}$ , respectively.  $\mathbf{A} \odot \mathbf{B}$  stands for the Hadamard product of  $\mathbf{A}$  and  $\mathbf{B}$ .  $\text{diag}(\mathbf{a})$  represents a square diagonal matrix with the elements of vector  $\mathbf{a}$  on the diagonal.  $\text{Re}(x)$  and  $\text{Im}(x)$  stand for the real and imaginary part of  $x$ , respectively.  $\text{Pr}[\cdot]$  denotes the probability.

## II. SYSTEM MODEL

Consider a MIMO system with one-bit quantization, as shown in Fig. 1. There are  $N_t$  antennas at the transmitter and  $N_r$  antennas at the receiver. Assuming perfect synchronization and a narrowband channel, the baseband received signal in this  $N_t \times N_r$  MIMO system is,

$$\mathbf{y} = \mathbf{H}\mathbf{x} + \mathbf{n} \quad (1)$$

where  $\mathbf{H} \in \mathbb{C}^{N_r \times N_t}$  is the channel matrix,  $\mathbf{x} \in \mathbb{C}^{N_t \times 1}$  is the signal sent by the transmitter,  $\mathbf{y} \in \mathbb{C}^{N_r \times 1}$  is the received signal before quantization, and  $\mathbf{n} \sim \mathcal{CN}(0, \mathbf{I})$  is the circularly symmetric complex Gaussian noise.

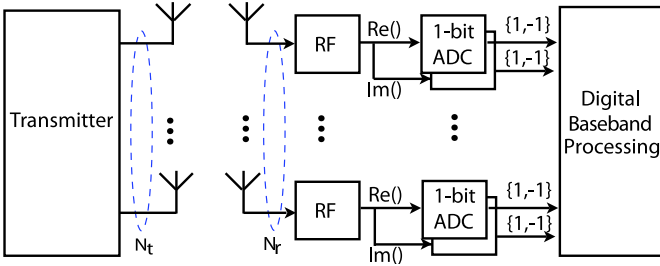


Fig. 1. A  $N_t \times N_r$  MIMO system with one-bit quantization at the receiver. For each receiver antenna, there are two one-bit ADCs. Note that there is no limitation on the structure of the transmitter.

In our system, there are a total of  $2N_r$  one-bit resolution quantizers that separately quantize the real and imaginary part of each received signal. The output after the one-bit quantization is

$$\mathbf{r} = \text{sgn}(\mathbf{y}) = \text{sgn}(\mathbf{H}\mathbf{x} + \mathbf{n}), \quad (2)$$

where  $\text{sgn}(\cdot)$  is the signum function applied componentwise on its input. Therefore, the quantization output at the  $i$ th antenna  $r_i \in \{1 + j, 1 - j, -1 + j, -1 - j\}$  for  $1 \leq i \leq N_r$ .

In this paper, we assume that there is both CSIT and CSIR. Consequently, the channel capacity with one-bit quantization is

$$C = \max_{p(\mathbf{x}) : \text{tr}(\mathbb{E}(\mathbf{x}\mathbf{x}^*)) \leq P_t} I(\mathbf{x}; \mathbf{r}|\mathbf{H}), \quad (3)$$

where

$$I(\mathbf{x}; \mathbf{r}|\mathbf{H}) = \int_{\mathbf{x}} \sum_{\mathbf{r}} \Pr(\mathbf{x}) \Pr(\mathbf{r}|\mathbf{x}) \log_2 \frac{\Pr(\mathbf{r}|\mathbf{x})}{\Pr(\mathbf{r})} d\mathbf{x}, \quad (4)$$

and  $P_t$  is the average power constraint at the transmitter.

### III. CAPACITY OF THE MIMO CHANNEL WITH ONE-BIT QUANTIZATION

The mutual information in (4) is in the form of multiple integrals. Obtaining a closed form expression for the optimization problem is a challenge. In this section, we derive an approximation of the channel capacity in the high SNR regime. For the simple SISO and MISO cases, we also find the capacity and the capacity-achieving strategy for any SNR. We start with the SISO case then move on to the MISO and MIMO cases.

#### A. SISO Channel with One-Bit Quantization

First, we deal with the very special case when  $N_t = N_r = 1$ . The channel coefficient now is a scalar denoted by  $h$ .

**Lemma 1.** *The capacity of the SISO channel with one-bit quantization is*

$$C_{1\text{bit},\text{SISO}} = 2 \left( 1 - H \left( Q \left( |h| \sqrt{P_t} \right) \right) \right), \quad (5)$$

where  $H(p) = -p \log_2 p - (1-p) \log_2 (1-p)$  and  $Q(\cdot)$  is the tail probability of the standard normal distribution and the capacity is achieved by rotated QPSK signaling with uniform probabilities, i.e.,

$$\Pr \left[ x = \sqrt{P_t} e^{j(k\pi + \frac{\pi}{4} - \angle h)} \right] = \frac{1}{4}, \text{ for } k = 0, 1, 2 \text{ and } 3. \quad (6)$$

*Proof:* Without loss of optimality, we can assume that the transmitted signal is  $x = e^{-j\angle h} \hat{x}$ . The outputs of the one-bit quantizer will be  $\text{Re}(r) = \text{sgn}(|h| \text{Re}(\hat{x}) + \text{Re}(n))$  and  $\text{Im}(r) = \text{sgn}(|h| \text{Im}(\hat{x}) + \text{Im}(n))$ . Therefore, the channel is decoupled into two real-valued channels with the same channel gain. For each real channel, it was proven in [17, Theorem 2] that binary antipodal signaling is optimal. Therefore, the optimal input for the SISO channel is rotated QPSK signaling. In addition, for the two real-valued equivalent channels, the capacity is  $1 - H(Q(|h| \sqrt{P_t}))$  [17, Theorem 2]. Therefore, the channel capacity is  $C_{1\text{bit},\text{SISO}} = 2(1 - H(Q(|h| \sqrt{P_t})))$ . ■

Since there are only two bits at the output of the quantizer, an upper bound on the capacity is 2 bps/Hz. When  $P_t \rightarrow \infty$ , it follows that  $Q(|h| \sqrt{P_t}) \rightarrow 0$  and  $C_{1\text{bit},\text{SISO}} \rightarrow 2$  bps/Hz. Therefore, the upper bound on the capacity can be approached in the high SNR regime.

#### B. MISO Channel with One-Bit Quantization

In this subsection, we consider the MISO channel with one bit quantization. The received signal is

$$r = \text{sgn}(y) = \text{sgn}(\mathbf{h}^* \mathbf{x} + n) \quad (7)$$

where  $\mathbf{h} \in \mathbb{C}^{N_t \times 1}$  is the channel vector. If perfect ADCs are used at the receiver, the capacity-achieving transmission strategy is to use maximal ratio transmission (MRT) beamforming and Gaussian signaling. In a system with one-bit ADCs, Gaussian signaling, it turns out, is not optimal.

**Proposition 1.** *The capacity of the MISO channel with one-bit quantization is*

$$C_{1\text{bit},\text{MISO}} = 2 \left( 1 - H \left( Q \left( \|\mathbf{h}\| \sqrt{P_t} \right) \right) \right), \quad (8)$$

and the capacity is obtained by MRT beamforming and QPSK signaling, i.e.,

$$\Pr \left[ \mathbf{x} = \sqrt{P_t} \frac{\mathbf{h}}{\|\mathbf{h}\|} e^{j(k\pi + \frac{\pi}{4})} \right] = \frac{1}{4}, \text{ for } k = 0, 1, 2 \text{ and } 3. \quad (9)$$

*Proof:* Assume that the transmitted symbol is  $\mathbf{x} = \mathbf{U}\mathbf{s}$  where  $\mathbf{U} \in \mathbb{C}^{N_t \times N_t}$  is a unitary matrix and  $\mathbf{s} = [s_1, s_2, \dots, s_{N_t}]^T \in \mathbb{C}^{N_t \times 1}$  is the information-bearing signal. Since  $\mathbf{s} \rightarrow \mathbf{U}\mathbf{s}$  is one-to-one mapping,  $I(\mathbf{s}; r) = I(\mathbf{U}\mathbf{s}; r) = I(\mathbf{x}; r)$ . Therefore, this assumption does not change the capacity. Assuming the unitary matrix  $\mathbf{U} = \left[ \frac{\mathbf{h}}{\|\mathbf{h}\|}, \overline{\mathbf{U}}_{N_t \times (N_t-1)} \right]$ , then  $r = \text{sgn}(\|\mathbf{h}\|s_1 + n)$  where  $s_1$  is the first element in  $\mathbf{s}$ . Therefore, the MISO channel is transformed to an equivalent SISO channel with channel gain  $\|\mathbf{h}\|$ . To maximize the mutual information, we set  $s_2 = s_3 = \dots = s_{N_t} = 0$  and  $\mathbb{E}[s_1 s_1^*] = P_t$ . Therefore,  $\mathbf{x} = \frac{\mathbf{h}}{\|\mathbf{h}\|} s_1$ . Then Proposition 1 is proved by using Lemma 1. ■

Similar to the SISO case,  $C_{1\text{bit},\text{MISO}}$  converges to the upper bound 2bps/Hz in the high SNR regime. In the low SNR

regime,

$$\begin{aligned}
& C_{1\text{bit},\text{MISO}} \\
\stackrel{(a)}{=} & 2 \left( 1 - H \left( \frac{1}{2} - \frac{1}{\sqrt{2\pi}} \|\mathbf{h}\| \sqrt{P_t} + o(\|\mathbf{h}\|^2 P_t) \right) \right) \\
\stackrel{(b)}{=} & 2 \left( 1 - \left( 1 - \frac{2}{\ln 2} \left( \frac{1}{\sqrt{2\pi}} \|\mathbf{h}\| \sqrt{P_t} \right)^2 \right. \right. \\
& \left. \left. + \frac{4}{3 \ln 2} \left( \frac{1}{\sqrt{2\pi}} \|\mathbf{h}\| \sqrt{P_t} \right)^4 + o(\|\mathbf{h}\|^4 P_t^2) \right) \right) \\
= & \frac{2 \|\mathbf{h}\|^2 P_t}{\pi \ln 2} - \frac{2 \|\mathbf{h}\|^4 P_t^2}{3\pi^2 \ln 2} + o(\|\mathbf{h}\|^4 P_t^2) \quad (10)
\end{aligned}$$

where (a) and (b) follow from  $Q(t) = \frac{1}{2} - \frac{1}{\sqrt{2\pi}}t + o(t^2)$  and  $H(\frac{1}{2} + t) = 1 - \frac{2}{\ln 2}t^2 + \frac{4}{3 \ln 2}t^4 + o(t^4)$ , respectively. Note that in the low SNR regime, the capacity of MISO channel without quantization is  $C_{\text{MISO}} = \log_2(1 + \|\mathbf{h}\|^2 P_t) = \frac{\|\mathbf{h}\|^2 P_t}{\ln 2} + o(P_t)$ . Therefore, in the MISO channel with CSIT, the one-bit quantization results in  $-1.96$  dB ( $\frac{2}{\pi}$ ) power loss. A similar result was reported in [23] but under the assumption of only CSIR.

When there is only CSIR, as shown in [23, Theorem 2], the achievable rate with independent QPSK signaling on each transmitter antenna is

$$R_{1\text{bit},\text{MISO}}^{\text{QPSK}} = \frac{2 \|\mathbf{h}\|^2 P_t}{\pi N_t \ln 2} + o(\|\mathbf{h}\|^2 P_t). \quad (11)$$

Comparing the first terms in (10) and (11), we can see that independent QPSK signaling results in  $1/N_t$  power loss compared to the optimal strategy on the first order of  $P_t$ . The reason is that the optimal strategy has the beamforming gain because of the CSIT.

### C. SIMO Channel with One-Bit Quantization

Now we consider the SIMO channel. With  $N_r$  antennas at the receiver, there are at most  $2^{2N_r}$  possible quantization outputs. Therefore,  $2N_r$  bps/Hz is a simple upper bound on the channel capacity. This upper bound, unfortunately, cannot be approached when  $N_r$  is larger than one. We provide a precise characterization in the following proposition.

**Proposition 2.** *The capacity of the SIMO channel with one-bit quantization at high SNR, denoted as  $\bar{C}_{1\text{bit},\text{SIMO}}$ , satisfies*

$$\log_2(4N_r) \leq \bar{C}_{1\text{bit},\text{SIMO}} \leq \log_2(4N_r + 1). \quad (12)$$

*Proof:* Denote the SIMO channel as  $\mathbf{h} = [h_1, h_2, \dots, h_{N_r}]^T$ . When the phase of the transmitted symbol  $x$  is around  $\angle x = k\pi/2 - \angle h_i$  ( $k = 0, 1, 2, 3$ ;  $i = 1, 2, \dots, N_r$ ), one element of the one-bit quantization output will change. There are at most  $4N_r$  such phases, denoted as  $\Phi = \{\phi_i, 1 \leq i \leq 4N_r\}$ . We usually assume that the channel coefficients are generated from continuous distribution. Then with probability one,  $\angle h_m \neq \angle h_n + k\pi/2, k \in \{0, 1, 2, 3\}$  for  $m \neq n$ . Therefore, we assume there are  $4N_r$  different phases.

Following the derivations in [16] and [18], it can be shown the high SNR capacity is achieved with transmit symbols from three categories:

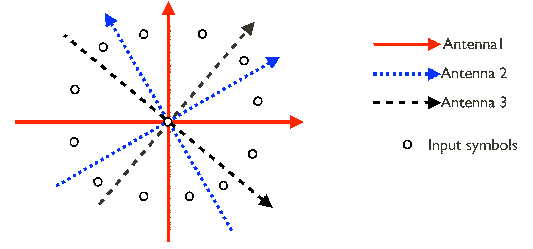


Fig. 2. The transmitted symbols of a SIMO channel with 3 receive antennas in the high SNR regime. Here,  $\angle h_1 = 0$  and  $\angle h_2 \neq \angle h_3 \neq 0$ . The optimal constellation contains 12 nonzero symbols and the symbol zero.

- 1) The symbol zero, i.e.,  $x = 0$ ;
- 2) The symbols with phases in  $\Phi$ ;
- 3) The symbols with phases not in  $\Phi$  (for instance, the input symbols shown in Fig. 2 except the symbol zero).

For the zero symbol, the transition probability  $\Pr[\mathbf{r}|x=0]$  is  $2^{-2N_r}$  for each possible  $\mathbf{r}$ . For the symbols with phases not in  $\Phi$ ,  $\Pr[\mathbf{r}|x] = \mathbf{1}_{\{\mathbf{r}=\mathbf{Q}(\mathbf{h}x)\}}$  where  $\mathbf{1}_{\{\cdot\}}$  is the indicator function. At last consider the symbols with phases in  $\Phi$ . If  $\angle x = -\angle h_1$ , then  $\Pr[r_1 = 1 + j|x] = \Pr[r_1 = 1 - j|x] = 1/2$ . The other conditional probabilities can be derived similarly. Therefore, the transition probability matrix from these three kinds of input symbols to the output, which has the dimension as  $(4N_r + 1) \times 2^{2N_r}$ , is

$$\Pr[\mathbf{r}|x] = \begin{bmatrix} 2^{-2N_r} & 2^{-2N_r} & \dots & 2^{-2N_r} \\ \mathbf{T}_{4N_r \times 4N_r} & \mathbf{0}_{4N_r \times (2^{2N_r} - 4N_r)} & & \\ \mathbf{I}_{4N_r \times 4N_r} & \mathbf{0}_{4N_r \times (2^{2N_r} - 4N_r)} & & \end{bmatrix} \quad (13)$$

where all the entries of the first row is  $2^{-2N_r}$  and  $\mathbf{T}$  is a  $4N_r \times 4N_r$  circulant matrix with the first row being  $[1/2, 1/2, 0, \dots, 0]$ .

Assume that these three kinds of symbols are transmitted with probabilities  $p_0$ ,  $p_1$  and  $1 - p_0 - p_1$ , respectively. The resulting mutual information is,

$$\begin{aligned}
f(p_0, p_1) & \triangleq \left( -1 + p_0 - p_1 - p_0 \frac{4N_r}{4N_r} \right) \\
& \times \log_2 \left( \frac{1 - p_0 - p_1}{4N_r} + \frac{p_0}{4N_r} + p_1 \right) - 2p_1 \\
& - \frac{8N_r^2}{4N_r} p_0 - \frac{4N_r - 4N_r}{4N_r} p_0 \log_2 p_0. \quad (14)
\end{aligned}$$

The channel capacity can be computed by searching the optimal  $p_0$  and  $p_1$ , denoted as  $p_0^*$  and  $p_1^*$ , which maximizes the mutual information  $f(p_0, p_1)$ . It turns out that  $\partial f(p_0, p_1)/\partial p_1 < 0$  and thus  $p_1^* = 0$ . Therefore, there are at most  $4N_r + 1$  possible input symbols in the capacity-achieving distribution and an upper bound on the capacity is  $\log_2(4N_r + 1)$ .

In Fig. 2, we show such an example when  $N_r = 3$ . The 6 axes represent the quantization thresholds of the 6 one-bit ADCs seen at the transmitter. The axes are offset due to the rotations induced by the channel coefficients. It is shown that the entire plane is divided into 12 regions. The optimal constellation contains 12 nonzero symbols falling in these regions and the symbol zero.

The lower bound  $\log_2(4N_r)$  is achieved by setting  $p_0 = 0$  and  $p_1 = 0$ , i.e.,  $f(0, 0) = \log_2(4N_r)$ . In other words, the

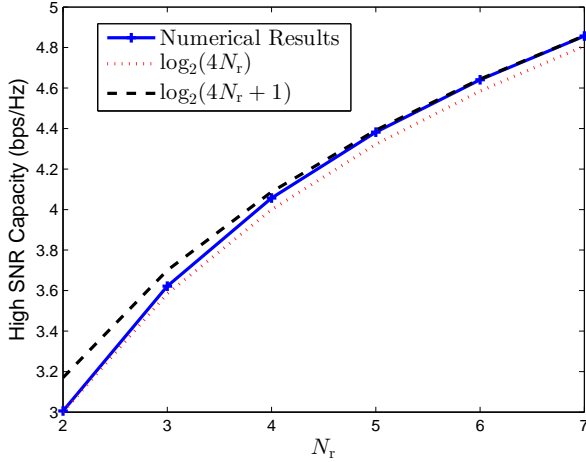


Fig. 3. The high SNR capacity and its lower and upper bounds. The high SNR capacity is very close to  $\log_2(4N_r + 1)$  when  $N_r \geq 6$ .

lower bound is achieved by transmitting the distinguishable  $4N_r$  symbols with equal probability. ■

**Corollary 1.** *When  $N_r$  is large, the capacity of the SIMO channel with one-bit quantization at high SNR is*

$$\bar{C}_{1\text{bit},\text{SIMO}} \approx \log_2(4N_r + 1). \quad (15)$$

*Proof:* In the proof of Proposition 2, we know that the optimal  $p_1$  is zero. From (14), the mutual information when  $p_1 = 0$  is,

$$\begin{aligned} f(p_0, 0) &= \left(-1 + p_0 - p_0 \frac{4N_r}{4N_r}\right) \log_2 \left(\frac{1-p_0}{4N_r} + \frac{p_0}{4N_r}\right) \\ &\quad - \frac{8N_r^2}{4N_r} p_0 - \frac{4N_r - 4N_r}{4N_r} p_0 \log_2 p_0. \end{aligned} \quad (16)$$

When  $N_r$  is large,  $\frac{N_r}{4N_r} \rightarrow 0$  and  $\frac{N_r^2}{4N_r} \rightarrow 0$ . Therefore,

$$f(p_0, 0) \approx -(1-p_0) \log_2 \frac{1-p_0}{4N_r} - p_0 \log_2 p_0. \quad (17)$$

It turns out that  $p_0^* = \frac{1}{4N_r+1}$  and  $f(p_0^*, 0) \approx \log_2(4N_r + 1)$ . ■

In Fig. 3, we plot the high SNR capacity obtained by numerically maximizing the mutual information function  $f(p_0, p_1)$ . The lower bound  $\log_2(4N_r)$  and upper bound  $\log_2(4N_r + 1)$  are also plotted. It is shown that the high SNR capacity converges to  $\log_2(4N_r + 1)$  when  $N_r \geq 6$ .

In communication systems, the zero symbol is often not included as part of the constellation due to peak-to-average power ratio (PAPR) issue. Therefore, in the high SNR regime, only  $4N_r$  distinguishable symbols are employed as the channel inputs and there will be  $4N_r$  different quantization outputs corresponding to each input symbol. The resulting achievable rate will converge to  $\log_2(4N_r)$  as transmission power increases.

In the SIMO channel, we can obtain the capacity-achieving input distribution using the cutting plane method [37, Sec. IV-A]. For this method, we take a fine quantized discrete grid on the region, for example,  $\{x : -3\sqrt{P_t} \leq \text{Re}(x) \leq 3\sqrt{P_t}, -3\sqrt{P_t} \leq \text{Im}(x) \leq 3\sqrt{P_t}\}$ , as the possible inputs and optimize their probabilities. Note that the capacity-achieving

input distribution may change with the SNR. In the simulations, this method is used to obtain the capacity of SIMO channel in the whole SNR regime.

#### D. MIMO Channel with One-Bit Quantization

In the high SNR regime, the decoding process at the receiver is as follows:

$$\mathbf{Find} \quad \mathbf{x} \quad (18a)$$

$$\text{s.t.} \quad \text{sgn}(\mathbf{H}\mathbf{x}) = \mathbf{r}, \quad (18b)$$

$$x \in \mathcal{X}, \quad (18c)$$

where  $\mathcal{X}$  is the set containing all the input symbols and the equation in (18b) is applied componentwise and separately to the real and imaginary parts. Therefore, the decoding process is similar to finding the input symbols satisfying a system of linear inequalities,

$$\text{sgn}(\mathbf{r}) \odot (\mathbf{H}\mathbf{x}) > 0. \quad (19)$$

where the Hadamard product and inequality are applied componentwise and separately to the real and imaginary parts. If there is only one input symbol satisfying the system of linear inequalities, it can be correctly decoded at high SNR. It turns out that the high SNR capacity of the quantized MIMO channel is closely related to a problem in classic combinatorial geometry. We first give a related lemma and its dual statement; the proof is available in several references e.g. [38]–[41].

**Lemma 2.**  *$N$  hyperplanes in general position passing through the origin of a  $d$  dimensional space divide the space into  $2 \sum_{k=0}^{d-1} \binom{N-1}{k}$  regions.*

**Dual:** *A  $d$  dimensional subspace in general position in  $N$  dimensional space intersects  $2 \sum_{k=0}^{d-1} \binom{N-1}{k}$  orthants.*

We first give two examples of the lemma. First, a line passing through the origin divides any dimensional space into 2 regions. Second,  $N$  distinct lines passing through the origin divide the 2-D plane into  $2 \binom{N-1}{0} + 2 \binom{N-1}{1} = 2N$  regions.

A set of  $N$  vectors is *in general position* in  $d$  dimensional space if and only if every subset of  $d$  or fewer vectors is linearly independent. If we put the  $N$  vectors, denoted as  $\mathbf{w}_1, \mathbf{w}_2, \dots, \mathbf{w}_N$ , into a matrix  $\mathbf{W}_{N \times d} = (\mathbf{w}_1, \mathbf{w}_2, \dots, \mathbf{w}_N)^T$ . These  $N$  vectors are *in general position* in  $d$ -dimensional space if and only if every  $d \times d$  submatrix has a nonzero determinant [40]. Note that general position is a strengthened rank condition<sup>1</sup>.

Based on Lemma 2, we provide our results on the MIMO channel capacity with one-bit quantization.

**Proposition 3.** *If the channel coefficients are independently generated from a continuous distribution, then the high SNR capacity satisfies*

$$\log_2(K(N_r, N_t)) \leq \bar{C}_{1\text{bit},\text{MIMO}} \leq \log_2(K(N_r, N_t) + 1) \quad (20)$$

<sup>1</sup>For example, the matrix  $\begin{pmatrix} 1 & 1 \\ 1 & 2 \\ 1 & 1 \end{pmatrix}$  has full column rank but does not satisfy the condition of general position.

where

$$K(N_r, N_t) \triangleq 2 \sum_{k=0}^{2N_t-1} \binom{2N_r-1}{k} \quad (21)$$

when  $N_t < N_r$  and

$$\bar{C}_{1\text{bit},\text{MIMO}} = 2N_r \quad (22)$$

when  $N_t \geq N_r$ .

*Proof:* Assuming there is no noise, the equivalent real-valued channel is

$$\hat{\mathbf{r}} = \text{sgn}(\hat{\mathbf{H}}\hat{\mathbf{x}}), \quad (23)$$

where  $\hat{\mathbf{x}} = [\text{Re}(\mathbf{x})^T, \text{Im}(\mathbf{x})^T]^T$ ,  $\hat{\mathbf{r}} = [\text{Re}(\mathbf{r})^T, \text{Im}(\mathbf{r})^T]^T$  and

$$\hat{\mathbf{H}}_{2N_r \times 2N_t} = \begin{bmatrix} \text{Re}(\mathbf{H}) & -\text{Im}(\mathbf{H}) \\ \text{Im}(\mathbf{H}) & \text{Re}(\mathbf{H}) \end{bmatrix}. \quad (24)$$

Each row of the channel matrix  $\hat{\mathbf{H}}$  defines a hyperplane passing through the origin of a  $2N_t$  dimensional space. These  $2N_r$  hyperplanes divide the  $2N_t$  dimensional space into  $2 \sum_{k=0}^{2N_t-1} \binom{2N_r-1}{k}$  regions. For the dual statement, the subspace spanned by the  $2N_t$  columns of  $\hat{\mathbf{H}}$  intersects  $2 \sum_{k=0}^{2N_t-1} \binom{2N_r-1}{k}$  orthants in the  $2N_r$  dimensional space. In other words, there are  $2 \sum_{k=0}^{2N_t-1} \binom{2N_r-1}{k}$  possible different  $\mathbf{r}$ 's by varying the transmitted symbol  $\mathbf{x}$ .

To achieve the channel capacity at high SNR, the transmitter has to send the zero symbol and  $2 \sum_{k=0}^{2N_t-1} \binom{2N_r-1}{k}$  symbols from each region. The proof is similar to the proof of Proposition 2. Note that when  $N_t \geq N_r$ , the transmitter can send  $2^{2N_r}$  symbols corresponding to all  $2^{2N_r}$  possible quantization outputs with equal probabilities  $2^{-2N_r}$ . Therefore, the zero symbol is not sent when  $N_t \geq N_r$ .

At last, we discuss the condition of ‘‘in general position’’ in Lemma 2. The  $2N_r$  hyperplanes defined by the matrix  $\hat{\mathbf{H}}_{2N_r \times 2N_t}$  are in general position if every  $2N_t \times 2N_t$  submatrix of  $\hat{\mathbf{H}}$  has a nonzero determinant. In this proposition, we assume the coefficients of  $\hat{\mathbf{H}}$  are independently generated from a continuous distribution. Therefore, with probability one, the condition of *general position* is satisfied. ■

The function  $K(N_r, N_t)$  has the following properties:

- 1)  $K(1, N_t) = 4$ ;
- 2)  $K(N_r, 1) = 4N_r$ .

Property 1 implies that the high SNR capacities of SISO and MISO channel are  $\log_2 K(1, N_t) = 2$  bps/Hz. Combining Property 2 and Proposition 3, we obtain that the high SNR capacity of SIMO channel is between  $\log_2(4N_r)$  and  $\log_2(4N_r + 1)$ , which is Proposition 2.

In Fig. 4 and Fig. 5, we plot  $\log_2 K(N_r, N_t)$ , which is very close to the high SNR capacity  $\bar{C}_{1\text{bit},\text{MIMO}}$  as shown in (20). In Fig. 4,  $\log_2 K(N_r, N_t)$  is a strictly increasing function of  $N_r$ . In Fig. 5, we see that  $\log_2 K(N_r, N_t)$  increases fast with  $N_t$  and quickly becomes saturated when  $N_t \geq \frac{N_r}{2}$ . When  $N_t \geq N_r$ ,  $\log_2 K(N_r, N_t) = 2N_r$ . Moreover, we see that  $K(m, n) \neq K(n, m)$  in general. This means that the capacity of a quantized  $m \times n$  channel is different from that of a quantized  $n \times m$  channel. This is in striking contrast with unquantized MIMO systems.

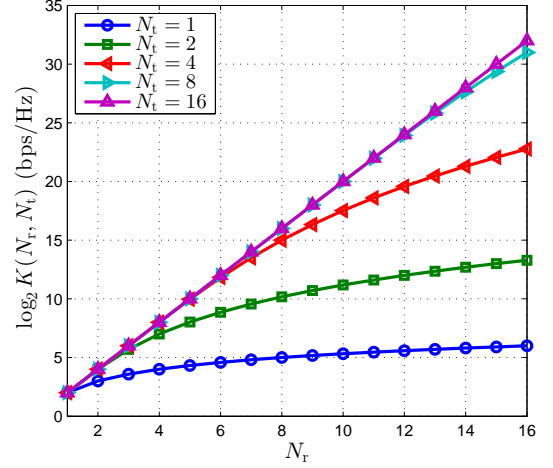


Fig. 4.  $\log_2 K(N_r, N_t)$  versus  $N_r$  for different  $N_t$ .  $K(N_r, N_t)$  is defined as  $2 \sum_{k=0}^{2N_t-1} \binom{2N_r-1}{k}$  and  $\log_2 K(N_r, N_t)$  is close to the high SNR capacity of the MIMO channel with  $N_t$  transmit antennas and  $N_r$  receive antennas.

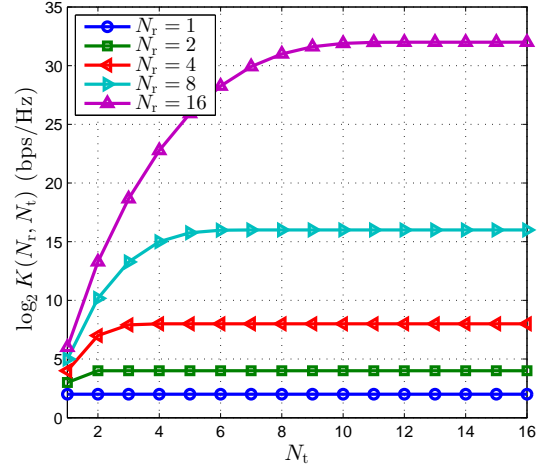


Fig. 5.  $\log_2 K(N_r, N_t)$  versus  $N_t$  for different  $N_r$ .  $K(N_r, N_t)$  is defined as  $2 \sum_{k=0}^{2N_t-1} \binom{2N_r-1}{k}$  and  $\log_2 K(N_r, N_t)$  is close to the high SNR capacity of the MIMO channel with  $N_t$  transmit antennas and  $N_r$  receive antennas.

#### IV. NUMERICAL INPUT OPTIMIZATION METHODS FOR THE MIMO CHANNEL AT HIGH SNR

In Section III, we derived the high SNR capacity of the MIMO channel  $\bar{C}_{1\text{bit},\text{MIMO}}$ . Unlike the SISO and MISO cases, the capacity-achieving input distribution is not known in closed-form. In addition, the cutting plane method used to optimize the input distribution in the SIMO channel does not apply to MIMO case since its complexity increases exponentially with the number of transmitter antennas. In this section, we propose two heuristic methods to design the transmitted constellation based on full knowledge of CSIT.

##### A. Channel Inversion

When  $\mathbf{H}\mathbf{H}^*$  is invertible, a simple transmission strategy is to use channel inversion (CI) precoding and QPSK signaling.

The transmitted symbol is

$$\mathbf{x} = \sqrt{\frac{P_t}{\text{tr}(\mathbf{H}\mathbf{H}^*)^{-1}}} \mathbf{H}^* (\mathbf{H}\mathbf{H}^*)^{-1} \mathbf{s}, \quad (25)$$

where  $\mathbf{s} \in \mathbb{C}^{N_r \times 1}$  is a vector with independent QPSK entries that satisfies  $\mathbb{E}[\mathbf{s}\mathbf{s}^*] = \mathbf{I}_{N_r \times N_r}$ . The expected transmission power is mounted as  $\mathbb{E}[\mathbf{x}\mathbf{x}^*] = P_t$ . The output of the quantizer with this choice of precoder is

$$\mathbf{r} = \text{sgn} \left( \sqrt{\frac{P_t}{\text{tr}(\mathbf{H}\mathbf{H}^*)^{-1}}} \mathbf{s} + \mathbf{n} \right). \quad (26)$$

The channel decomposes into  $N_r$  parallel one-bit quantized SISO channels with same channel gain. According to Lemma 1, the achievable rate is

$$R_{1\text{bit}}^{\text{CI}} = 2N_r \left( 1 - H \left( Q \left( \sqrt{\frac{P_t}{\text{tr}(\mathbf{H}\mathbf{H}^*)^{-1}}} \right) \right) \right). \quad (27)$$

As  $N_r \rightarrow +\infty$  and  $N_t/N_r = c$  ( $c$  is a constant larger than 1), the following convergence holds almost surely [42],

$$\frac{1}{N_r} \text{tr}(\mathbf{H}\mathbf{H}^*)^{-1} \rightarrow \frac{1}{N_t - N_r}. \quad (28)$$

Therefore, we have

$$\hat{R}_{1\text{bit}}^{\text{CI}} \triangleq \lim_{N_r \rightarrow +\infty, N_t/N_r = c} R_{1\text{bit}}^{\text{CI}} \quad (29)$$

$$= 2N_r \left( 1 - H \left( Q \left( \sqrt{\left( \frac{N_t}{N_r} - 1 \right) P_t} \right) \right) \right). \quad (30)$$

Since  $H(Q(x))$  is a decreasing function when  $x > 0$ ,  $\hat{R}_{1\text{bit}}^{\text{CI}}$  increases with the ratio  $\frac{N_t}{N_r}$ .

In Fig. 6, we plot  $\hat{R}_{1\text{bit}}^{\text{CI}}$  and the average achievable rate  $\bar{R}_{1\text{bit}}^{\text{CI}}$  which is

$$\bar{R}_{1\text{bit}}^{\text{CI}} = \mathbb{E} \left[ 2N_r \left( 1 - H \left( Q \left( \sqrt{\frac{P_t}{\text{tr}(\mathbf{H}\mathbf{H}^*)^{-1}}} \right) \right) \right) \right] \quad (31)$$

The channel matrix  $\mathbf{H}$  is assumed to have IID Gaussian entries. It shows that  $\bar{R}_{1\text{bit}}^{\text{CI}}$  and  $\hat{R}_{1\text{bit}}^{\text{CI}}$  is very close when  $N_r = 8$  and almost overlap when  $N_t \geq 16$ .

Next, we discuss the properties of  $R_{1\text{bit}}^{\text{CI}}$  at high and low SNR. In (27), we see that  $R_{1\text{bit}}^{\text{CI}}$  converges to  $2N_r$  bps/Hz at high SNR, which is same as  $\bar{C}_{1\text{bit}, \text{MIMO}}$ . In Fig. 6,  $R_{1\text{bit}}^{\text{CI}}$  converges to  $2N_r = 8$  bps/Hz. Moreover, we find that  $R_{1\text{bit}}^{\text{CI}}$  converges when the SNR is merely larger than 0 dB and -5 dB when  $N_t = 64$  and 256, respectively. This means that the ‘‘high SNR’’ in our analysis can be in the low SNR regime in practice. Furthermore,  $H(Q(2.23)) \approx 0.1$ , thus when

$$P_t \approx \frac{2.23^2}{N_t/N_r - 1} \approx \frac{5.0}{N_t/N_r - 1}, \quad (32)$$

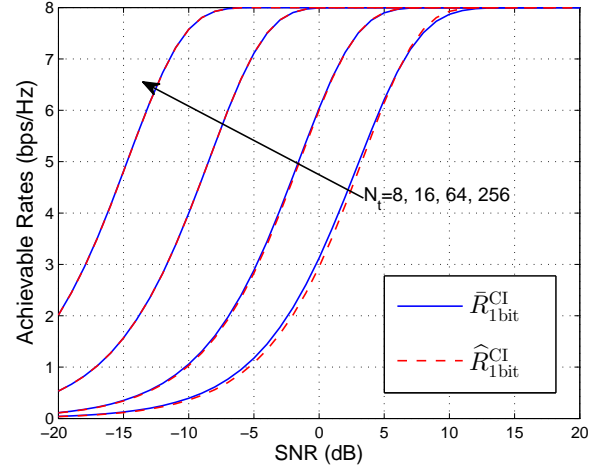


Fig. 6. The achievable rates by channel inversion method.  $N_r = 4$  and  $N_t$  is increased from 8 to 256.  $\bar{R}_{1\text{bit}}^{\text{CI}}$  is obtained by averaging over 1000 channel realizations where the channel matrix has IID Gaussian entries.

90% of the maximum rate, i.e.,  $1.8N_r$  bps/Hz, can be achieved. For example, when  $N_t/N_r \geq 6$ , the rate  $1.8N_r$  bps/Hz is achieved when  $P_t = 1$  or the SNR is 0 dB.

If the channel  $\mathbf{H}$  has IID complex Gaussian entries, the matrix  $\mathbf{H}\mathbf{H}^*$  is invertible with probability one when  $N_t \geq N_r$ . Denote the eigenvalues of  $\mathbf{H}\mathbf{H}^*$  as  $\lambda_1 \geq \lambda_2 \geq \dots \geq \lambda_{N_r} > 0$ . At low SNR, we have

$$R_{1\text{bit}}^{\text{CI}} = \frac{2}{\pi} \frac{N_r P_t}{\text{tr}(\mathbf{H}\mathbf{H}^*)^{-1} \ln 2} + o(P_t) \quad (33)$$

$$= \frac{2}{\pi} \frac{N_r}{\frac{1}{\lambda_1} + \frac{1}{\lambda_2} + \dots + \frac{1}{\lambda_{N_r}}} \frac{P_t}{\ln 2} + o(P_t), \quad (34)$$

and

$$\mathbb{E}[R_{1\text{bit}}^{\text{CI}}] \stackrel{(a)}{>} \frac{2(N_t - N_r) P_t}{\pi \ln 2} + o(P_t), \quad (35)$$

where (a) follows from  $\mathbb{E}[\text{tr}(\mathbf{H}\mathbf{H}^*)^{-1}] = \frac{N_r}{N_t - N_r}$  when  $N_t > N_r$  [43] and Jensen’s inequality. In [23, Theorem 2], the achievable rate of MIMO channel with independent QPSK signaling and one-bit ADCs at low SNR is shown to be

$$R_{1\text{bit}}^{\text{QPSK}} = \frac{2}{\pi} \text{tr}(\mathbf{H}\mathbf{H}^*) \frac{P_t}{N_t \ln 2} + o(P_t) \quad (36)$$

$$= \frac{2}{\pi} \frac{\lambda_1 + \lambda_2 + \dots + \lambda_{N_r}}{N_t} \frac{P_t}{\ln 2} + o(P_t), \quad (37)$$

and

$$\mathbb{E}[R_{1\text{bit}}^{\text{QPSK}}] \stackrel{(a)}{=} \frac{2N_r}{\pi} \frac{P_t}{\ln 2} + o(P_t), \quad (38)$$

where (a) follows from  $\mathbb{E}[\text{tr}(\mathbf{H}\mathbf{H}^*)] = N_t N_r$  [43].

When  $N_r = N_t$ ,  $R_{1\text{bit}}^{\text{QPSK}} \geq R_{1\text{bit}}^{\text{CI}}$  because of Jensen’s inequality  $\frac{1}{\mathbb{E}(x)} \leq \mathbb{E}\left(\frac{1}{x}\right)$ . This means that with relative small transmitter antenna array, the channel inversion method does not provide gain over the simple QPSK signalling. However, if  $N_t \geq 2N_r$ , then  $R_{1\text{bit}}^{\text{QPSK}} < R_{1\text{bit}}^{\text{CI}}$ . The reason is that the

channel inversion strategy has precoding gain which increases with the number of transmitter antennas.

### B. Convex Optimization

The channel inversion strategy only applies when  $\mathbf{H}\mathbf{H}^*$  is invertible (or  $N_t \geq N_r$  when  $\mathbf{H}$  has IID Gaussian entries). In this subsection, we propose another heuristic method that achieves the high SNR capacity  $\bar{C}_{1\text{bit},\text{MIMO}}$  without requiring  $\mathbf{H}\mathbf{H}^*$  being invertible. The basic idea is: for each possible quantization output  $\mathbf{r}$ , find the input signal  $\mathbf{x}$  such that  $\mathbf{r} = \text{sgn}(\mathbf{H}\mathbf{x})$ .

The input signals  $\mathbf{x}$  are obtained by solving the following optimization problem,

$$\mathbf{P1:} \quad \max_{\mathbf{x}} \quad d \quad (39a)$$

$$\text{s.t.} \quad \mathbf{Re}(\mathbf{H}\mathbf{x}) \odot \mathbf{Re}(\mathbf{r}) \geq d, \quad (39b)$$

$$\mathbf{Im}(\mathbf{H}\mathbf{x}) \odot \mathbf{Re}(\mathbf{r}) \geq d, \quad (39c)$$

$$\text{sgn}(\mathbf{H}\mathbf{x}) = \mathbf{r}, \quad (39d)$$

$$\mathbf{x}^* \mathbf{x} \leq P_t. \quad (39e)$$

where the inequalities  $\geq$  in (39b) and (39c) are applied componentwise. The objective is to maximize the minimum distance between the noiseless received signal  $\mathbf{H}\mathbf{x}$  and the threshold of the one-bit ADCs, which is zero.

Using the notation given in (23), we rewrite Problem **P1** in a compact form as,

$$\mathbf{P2:} \quad \max_{\hat{\mathbf{r}}} \quad d \quad (40a)$$

$$\text{s.t.} \quad \left( \text{diag}(\hat{\mathbf{r}}) \hat{\mathbf{H}} \right) \hat{\mathbf{x}} \geq d, \quad (40b)$$

$$\hat{\mathbf{x}}^T \hat{\mathbf{x}} \leq P_t. \quad (40c)$$

For fixed  $\hat{\mathbf{r}}$ , the inequality constraint (40b) is linear and thus convex. Therefore, the problem **P2** is convex and can be efficiently solved [44]. There are a total of  $2^{2N_r}$  possible values of  $\hat{\mathbf{r}}$  and thus  $2^{2N_r}$  different optimization problems.

Denote the optimal value of Problem **P2** as  $d^*(\hat{\mathbf{r}})$ . Note that if  $\hat{\mathbf{x}} = \mathbf{0}$ , the value of the objective function in Problem **P2** is zero regardless of  $\hat{\mathbf{r}}$ . Therefore, a lower bound of  $d^*(\hat{\mathbf{r}})$  is zero. We can see that  $d^*(\hat{\mathbf{r}}) > 0$  if and only if there exists  $\hat{\mathbf{x}}$  satisfying

$$\left( \text{diag}(\hat{\mathbf{r}}) \hat{\mathbf{H}} \right) \hat{\mathbf{x}} > \mathbf{0}. \quad (41)$$

Therefore, it is possible to check the feasibility of (41) before solving the optimization problem. Actually, (41) is a system of linear inequalities. Analogous to the rank condition for the feasibility of the system of linear equalities, there is a similar condition for the feasibility of the system of the linear inequalities. A sufficient and necessary condition that a solution of (41) exists is that the *inequality-rank* (*I-rank*) of the matrix  $\left( \text{diag}(\hat{\mathbf{r}}) \hat{\mathbf{H}} \right)$  be greater than zero [45] (see [45] for more details about the definition and computation of the *I-rank*).

The transmitter constellation is composed of the nonzero solutions of the  $2^{2N_r}$  convex optimization problems and the zero symbol. To reduce the PAPR, the zero symbol is often not included in the constellation. Therefore, in our simulations, the

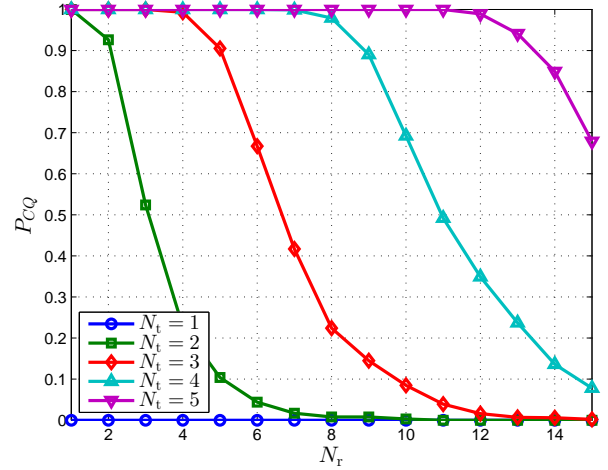


Fig. 7.  $P_{CQ}$  versus  $N_r$  in the MIMO system with one-bit ADCs and QPSK signaling for different  $N_t$ .  $P_{CQ}$  is very large when  $N_r$  is not large enough.

transmitter constellation only contains the nonzero solutions of the convex optimization problems. Instead of transmitting the symbols with equal probability, we can also optimize the probabilities of each symbol using the well-known Blahut-Arimoto algorithm [46]. The performance improvement is shown in our simulation results. We find that optimization of the transmission probability of the symbols only provides small gain over a uniform distribution in the low and medium SNR regime.

### C. Stochastic Resonance in Coarsely Quantized Channel

In the MIMO channel, if the constellation of the input symbols is not carefully designed, it is possible that there exists transmitted symbols  $\mathbf{x}_1$  and  $\mathbf{x}_2$  ( $\mathbf{x}_1 \neq \mathbf{x}_2$ ) such that  $\text{sgn}(\mathbf{H}\mathbf{x}_1) = \text{sgn}(\mathbf{H}\mathbf{x}_2)$ . In [21] and [22], such MIMO systems with indistinguishable inputs are called *coarsely quantized*. When the noise power is reduced to zero, the receiver cannot distinguish  $\mathbf{x}_1$  and  $\mathbf{x}_2$ . However, it is possible that  $\text{sgn}(\mathbf{H}\mathbf{x}_1 + \mathbf{n}) \neq \text{sgn}(\mathbf{H}\mathbf{x}_2 + \mathbf{n})$  in the noisy channel and thus  $\mathbf{x}_1$  and  $\mathbf{x}_2$  can be separated by the receiver. Whether the MIMO system is coarsely quantized depends on both the channel  $\mathbf{H}$  and the transmitted symbols. Here, we provide one example.

**Example 1.** For a MIMO channel without CSIT, suppose that QPSK signaling is used at each transmitter antenna. Therefore there are  $2^{2N_t}$  possible transmitted symbols and  $2^{2N_r}$  possible quantization outputs. The channel gain  $\mathbf{H}$  is assumed to have IID Gaussian entries. The probability that the MIMO system is coarsely quantized, denoted as  $P_{CQ}$ , is plotted in Fig. 7.  $P_{CQ}$  increases with  $N_t$  and decreases with  $N_r$ . If  $N_t = 1$ , then  $P_{CQ} = 0$  which means that all the four possible inputs can be separated at the receiver. When  $N_t > 1$ , we see that  $P_{CQ}$  is very large. For example, when  $N_t = N_r = 2$ , the receiver cannot distinguish the 16 possible inputs with the probability as high as 0.9. When  $N_t = 4$ , at least 11 receiver antennas are needed to ensure that  $P_{CQ} < 0.5$ .



An interesting phenomenon that may happen in the coarsely quantized MIMO channel is called *stochastic resonance* [18], [22]. The broadest definition of stochastic resonance is that it occurs when randomness may have some positive role in a signal processing context [47]. When stochastic resonance occurs, the mutual information will first increase with the transmitter power  $P_t$  to a maximum, then decreases with  $P_t$ , and finally converges. In other words, there is an optimal SNR below infinity. This is in contrast with results in the continuous-output MIMO channel where the capacity increases monotonically with  $P_t$ . A simple explanation is that one-bit quantization is a nonlinear operation. Noise can be helpful in such nonlinear systems [48].

If the MIMO system is coarsely quantized, there may be loss of achievable rate at high SNR. Consider a coarsely quantized  $N \times N$  MIMO system with QPSK signaling as an example. In this system, at least 2 of the  $2^{2N}$  inputs result in the same output at high SNR and the number of possible outputs is less than  $2^{2N}$ . Therefore, the achievable rate is less than  $2N$  bps/Hz. In our proposed methods, the achievable rate at high SNR is  $2N$  bps/Hz. The large  $P_{CQ}$  implies that with high probability our proposed methods have better performance than QPSK signaling at high SNR.

## V. MMWAVE CHANNEL WITH ONE-BIT QUANTIZATION

In mmWave communications, the channel matrix  $\mathbf{H}$  is usually assumed to be low rank due to sparse scattering in the channel [49] and therefore does not satisfy the strict condition of *general position* in Proposition 3. As a result, we cannot directly obtain the high SNR capacity of the mmWave channel.

In this section, the mmWave MIMO channel is modelled using a ray-based model with  $L$  paths. We also assume that uniform planar arrays (UPA) in the  $yz$ -plane are deployed at the transmitter and receiver. Denote  $\alpha_\ell$ ,  $\varphi_{r\ell}$  ( $\theta_{r\ell}$ ),  $\varphi_{t\ell}$  ( $\theta_{t\ell}$ ) as the strengths, the azimuth (elevation) angles of arrival and the angle of departure of the  $\ell$ th path, respectively. The array response vectors at the transmitter or receiver is given by [50]

$$\mathbf{a}(\varphi, \theta) = \frac{1}{\sqrt{N}} [1, e^{jk(m \sin(\varphi) \sin(\theta) + n \cos(\theta))}, \dots, e^{jk((Y-1) \sin(\varphi) \sin(\theta) + (Z-1) \cos(\theta))}]^T, \quad (42)$$

where  $0 \leq m < Y$  and  $0 \leq n < Z$  are the  $y$  and  $z$  indices of an antenna element respectively. Herein,  $k = \frac{2\pi}{\lambda}d$  where  $\lambda$  is the wavelength and  $d$  is the inter-element spacing. Hence, the channel matrix is,

$$\mathbf{H} = \sum_{\ell=1}^L \alpha_\ell \mathbf{a}_r(\varphi_{r\ell}, \theta_{r\ell}) \mathbf{a}_t^*(\varphi_{t\ell}, \theta_{t\ell}) \quad (43)$$

$$= \mathbf{A}_r \mathbf{\Sigma} \mathbf{A}_t^* \quad (44)$$

where  $\mathbf{A}_r = [\mathbf{a}_r(\varphi_{r1}, \theta_{r1}), \mathbf{a}_r(\varphi_{r2}, \theta_{r2}), \dots, \mathbf{a}_r(\varphi_{rL}, \theta_{rL})]$ ,  $\mathbf{\Sigma} = \text{diag}(\alpha_1, \alpha_2, \dots, \alpha_L)$  and  $\mathbf{A}_t = [\mathbf{a}_t(\varphi_{t1}, \theta_{t1}), \mathbf{a}_t(\varphi_{t2}, \theta_{t2}), \dots, \mathbf{a}_t(\varphi_{tL}, \theta_{tL})]$ .

The number of multipaths tends to be lower in the mmWave band compared with lower frequencies. Meanwhile, large antenna arrays are usually deployed to obtain beamforming gain for combatting the path loss. Hence, we suppose that  $L < \min\{N_t, N_r\}$  in mmWave MIMO channels.

**Corollary 2.** For a mmWave MIMO system with  $L$  ( $L < \min(N_r, N_t)$ ) paths and one-bit quantization, the high SNR capacity satisfies,

$$\log_2(K(N_r, L)) \leq \overline{C}_{1\text{bit,mmW}} \leq \log_2(K(N_r, L) + 1). \quad (45)$$

*Proof:* First denote

$$\widehat{\mathbf{A}}_r = \begin{pmatrix} \mathbf{Re}(\mathbf{A}_t) & -\mathbf{Im}(\mathbf{A}_t) \\ \mathbf{Im}(\mathbf{A}_t) & \mathbf{Re}(\mathbf{A}_t) \end{pmatrix}. \quad (46)$$

When  $L \leq N_r$ , any  $2L \times 2L$  submatrix of  $\widehat{\mathbf{A}}_r$  has full rank with probability one since  $\varphi_{r\ell}$  and  $\theta_{r\ell}$  are generated from continuous distribution. Therefore,  $\mathbf{A}_r$  satisfies the condition of general position.

In addition,  $\mathbf{A}_t$  has rank  $L$  with probability one and thus  $\{\mathbf{A}_t^* \mathbf{x} : \mathbf{x} \in \mathbb{C}^{N_t \times 1}\}$  represents the  $L$ -dimensional complex space. Therefore, the channel is equivalent to a  $N_r \times L$  channel satisfying the condition of general position. Combining these with Proposition 3, we obtain Corollary 2. ■

Corollary 2 shows that multipath is helpful in improving the high SNR capacity in mmWave MIMO systems.

As  $\mathbf{H}\mathbf{H}^*$  is not invertible in mmWave systems, the channel inversion approach cannot be used to design the transmitted symbols. Instead, the convex optimization approach proposed in Section IV-B has to be used. We first write the singular value decomposition of the channel matrix as

$$\mathbf{H} = \mathbf{U}\mathbf{\Lambda}\mathbf{V}^*, \quad (47)$$

where  $\mathbf{\Lambda}_{L \times L}$  is a diagonal matrix,  $\mathbf{U}_{N_r \times L}$  and  $\mathbf{V}_{N_t \times L}$  are semi-unitary matrices. Then we solve the optimization problem similar to **P1**,

$$\mathbf{P3:} \quad \max_{\mathbf{z}} \quad d \quad (48a)$$

$$\text{s.t.} \quad \mathbf{Re}(\mathbf{U}\mathbf{\Lambda}\mathbf{z}) \odot \mathbf{Re}(\mathbf{r}) \geq d \quad (48b)$$

$$\mathbf{Im}(\mathbf{U}\mathbf{\Lambda}\mathbf{z}) \odot \mathbf{Im}(\mathbf{r}) \geq d \quad (48c)$$

$$\text{sgn}(\mathbf{U}\mathbf{\Lambda}\mathbf{z}) = \mathbf{r} \quad (48d)$$

$$\mathbf{z}^* \mathbf{z} \leq P_t. \quad (48e)$$

If the optimal solution is  $\mathbf{z}^*$ , the transmitted symbol is  $\mathbf{x} = \mathbf{V}\mathbf{z}^*$ . Since  $\mathbf{V}$  is semi-unitary, the power constraint is satisfied, i.e.,  $\mathbf{x}^* \mathbf{x} \leq P_t$ .

Next, to provide an intuition, we consider a mmWave MIMO channel with only one path and propose a capacity-achieving transmission strategy. If  $L = 1$ , the channel in (44) degenerates to

$$\mathbf{H} = \alpha \mathbf{a}_r(\varphi_r, \theta_r) \mathbf{a}_t^*(\varphi_t, \theta_t). \quad (49)$$

Following the same logic in the MISO setting, matched filter beamforming is used at the transmitter to obtain the beamforming gain. The resulting channel is equivalent to a SIMO channel with channel coefficients as  $\mathbf{h} = \alpha \|\mathbf{a}_t(\varphi_t, \theta_t)\|^2 \mathbf{a}_r(\varphi_r, \theta_r)$ . Then the cutting plane method can be used to design the transmitted symbols. Therefore, the transmitted symbols will be

$$\mathbf{x} = \mathbf{a}_t(\varphi_t, \theta_t) s \quad (50)$$

where  $s$  is the symbol obtained by the cutting plane method in the equivalent SIMO channel.

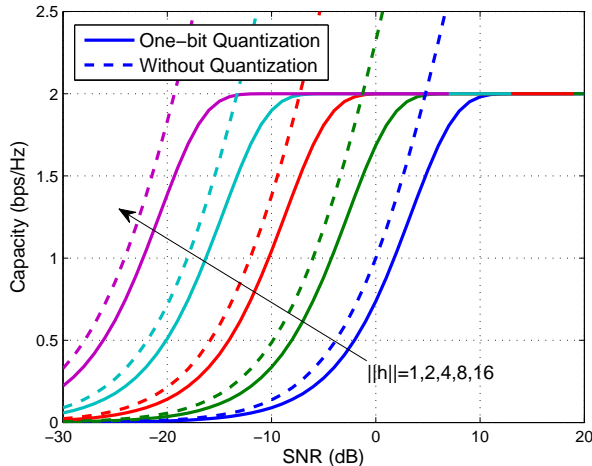


Fig. 8. Comparison of MISO channel capacity with one-bit quantization and that without quantization for different  $\|\mathbf{h}\|$ 's.

## VI. SIMULATION RESULTS

In this section, we first present simulation results of the capacities or achievable rates of the SIMO, MISO and the general MIMO channel at high and low SNR. The performance of the two proposed methods will also be compared. Then we consider the mmWave channel model and evaluate the achievable rates.

### A. MISO Channel with One-Bit Quantization

In Fig. 8, we plot the MISO channel capacity with and without one-bit quantization for different values of  $\|\mathbf{h}\|$ . First, we see that the channel capacity with one-bit quantization approaches 2 bps/Hz in the high SNR regime. Second, the transmitter antenna array provides power gain as shown in the figure. There is about 2 dB power loss in the low and medium SNR regimes, which verifies our analysis in (10). Third, when  $\|\mathbf{h}\| = 16$ , the capacity is close to the upper bound when SNR is larger than  $-15$  dB. We see that the “high SNR” in our analysis can be very low in the practice thanks to the beamforming gain provided by the multiple antennas.

### B. SIMO Channel with One-Bit Quantization

In the SIMO channel, we obtain the capacity-achieving input distribution using the cutting plane method. For this method, we take a fine quantized discrete grid on the region  $\{x : -3\sqrt{P_t} \leq \text{Re}(x) \leq 3\sqrt{P_t}, -3\sqrt{P_t} \leq \text{Im}(x) \leq 3\sqrt{P_t}\}$  as the possible inputs and optimize their probabilities. In Fig. 9, we show a simple case when  $\mathbf{h} = [e^{j\pi/8}, e^{-j\pi/8}]^T$ . It is interesting to find that the optimal input constellation contains the rotated 8-PSK symbols and the symbol zero. For other general channels, the optimal constellation may not be regular. For example, in Fig. 10, we show the optimal input distribution when  $\mathbf{h} = [1, 2e^{j\pi/3}]^T$ .

### C. MIMO Channel with One-Bit Quantization

In this part, we illustrate the average achievable rates of MIMO system with one-bit quantization. The channel coefficients are generated from  $\mathcal{CN}(0, 1)$  distribution independently

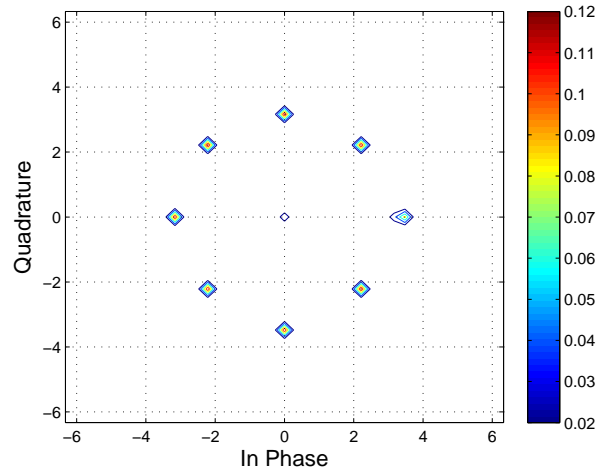


Fig. 9. The optimal input distribution of the SIMO channel where  $\mathbf{h} = [e^{j\pi/8}, e^{-j\pi/8}]^T$ . The transmission power  $P_t = 10$  and the achieved rate is about 2.52 bps/Hz.

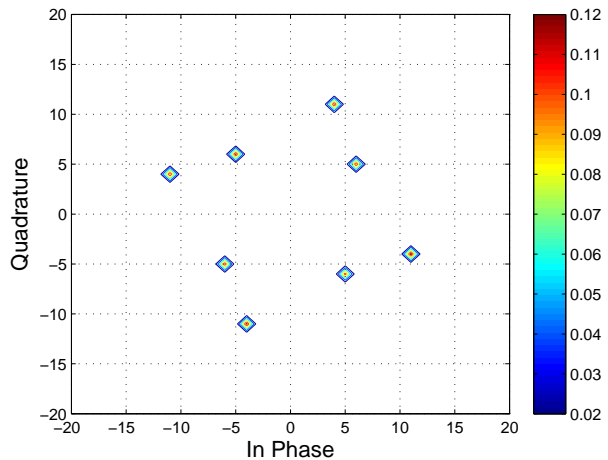


Fig. 10. The optimal input distribution of the SIMO channel where  $\mathbf{h} = [1, 2e^{j\pi/3}]^T$ . The transmission power  $P_t = 20$  dB and the achievable rate is 3.0050 bps/Hz.

and the results are obtained by averaging over 100 different channel realizations. The input alphabet, which contains  $2^{2N_r}$  input symbols, are constructed by the two proposed methods, i.e., channel inversion method and convex optimization method. For the convex optimization method, these symbols are transmitted with equal probabilities  $2^{-2N_r}$  or with probabilities optimized by the Blahut-Arimoto algorithm (denoted as “BA” in the figures). In these figures, we also plot the achievable rates when independent QPSK symbols across the antennas are transmitted at the transmitter.

In Figs. 11 and 12, we plot the achievable rates in the medium and high SNR regimes when  $N_t = N_r = 2$  and  $N_t = 2N_r = 4$ , respectively. The achievable rates with one-bit quantization converges to the upper bound 4 bps/Hz at high SNR. The rates of the channel without quantization are computed using the usual waterfilling approach. We can see that the power loss of the quantized systems compared

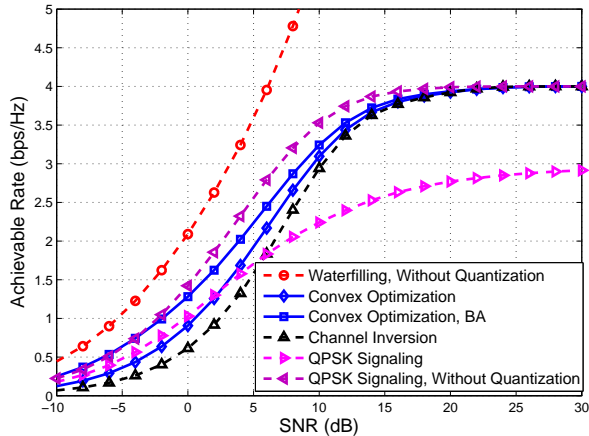


Fig. 11. Achievable rate of the  $2 \times 2$  MIMO system with one-bit ADCs in the medium and high SNR regimes.

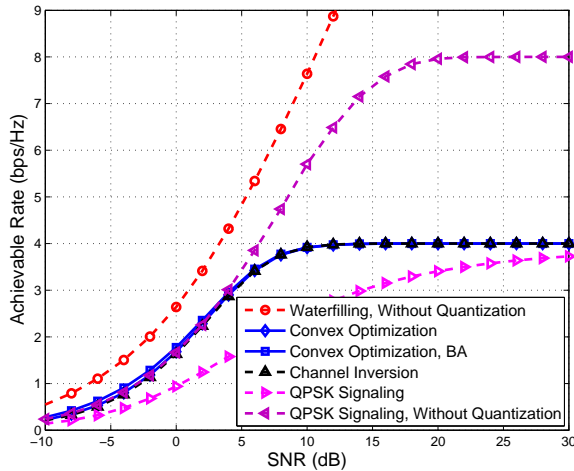


Fig. 12. Achievable rate of the  $4 \times 2$  MIMO system with one-bit ADCs in the medium and high SNR regimes.

to the unquantized systems is less than 5 dB at medium SNR. The channel inversion method works well at high SNR but has worse performance in the medium and low SNR regimes compared to the convex optimization method. But when  $N_r = 4$ , the gap between the performances of these two methods is negligible. For the case of independent QPSK signaling and one-bit quantization, we find that its rate is less than the two proposed methods at high SNR. As shown in Fig. 7, the  $2 \times 2$  and  $4 \times 2$  MIMO systems with QPSK signaling are coarsely quantized with high probability and the number of distinguishable inputs is less than the two proposed methods. Therefore, it has worse performance at high SNR. We also demonstrate the rates for QPSK signaling and without quantization where the input is discrete and the output is continuous. In the medium SNR, we see that the rate is close to the cases with one-bit quantization where the channel has discrete input and discrete output. However, in the high SNR regime, the rate will converge to  $\log_2(4^{N_t}) = 2N_t$  bps/Hz, instead of  $2N_r$  bps/Hz in the cases of one-bit quantization.

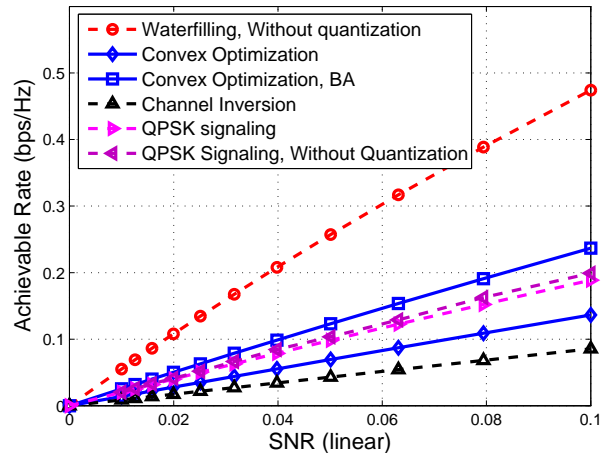


Fig. 13. Achievable rate of the  $2 \times 2$  MIMO system with one-bit ADCs in the low SNR regime ( $< -10$  dB). Note the SNR is in linear scale.

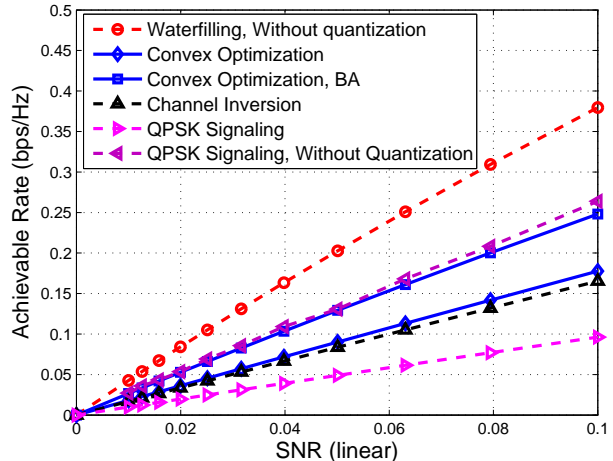


Fig. 14. Achievable rate of the  $4 \times 2$  MIMO system with one-bit ADCs in the low SNR regime ( $< -10$  dB). Note the SNR is in linear scale.

In Figs. 13 and 14, the achievable rates at the low SNR regime (below  $-10$  dB) are plotted versus the SNR in linear scale. The slopes of these curves can thus be easily identified to verify our analysis in Section IV-A. For the independent QPSK signaling, we plot the low SNR capacity approximation given by (36). When  $N_r = N_t = 2$ , we find that the channel inversion method is worse than the QPSK signaling. However, the channel inversion method is better when  $N_t = 2N_r = 4$ . This verifies our analysis in Section IV-A.

As shown in Figs. 11-14, optimizing the probabilities by the Blahut-Arimoto algorithm does not improve the achievable rates at the high SNR but provides gain at low and medium SNR. The convex optimization method with probabilities optimized by Blahut-Arimoto algorithm achieves the largest rate in the cases with one-bit quantization. The channel inversion method has lower complexity than convex optimization method but also worse performance.

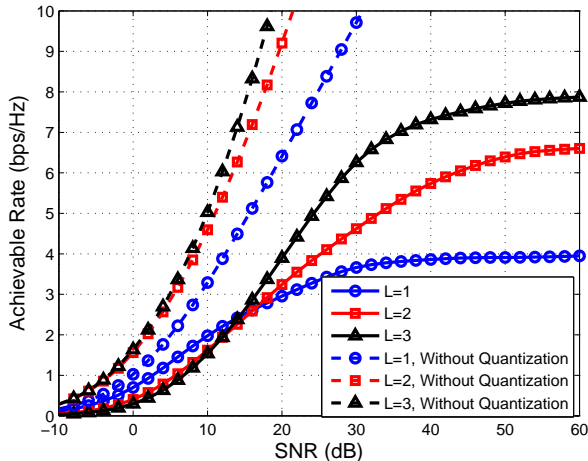


Fig. 15. The achievable rate of the mmWave  $256 \times 4$  mmWave system with different number of paths.  $16 \times 16$  and  $2 \times 2$  planar antenna arrays are installed at the transmitter and receiver, respectively. The inter-element spacing is one half of the wavelength.

#### D. MmWave Channel with One-Bit Quantization

We show the achievable rates in a  $256 \times 4$  channel with varying number of paths in Fig. 15. The azimuth angles  $(\varphi_t, \varphi_r)$  and elevation angles  $(\theta_t, \theta_r)$  are uniformly distributed over  $[0, 2\pi]$  and  $[-\pi/2, \pi/2]$ , respectively. The complex path gains  $\alpha$  are complex Gaussian variables. The inter-element spacing of the receiver antenna array is set to one half of the wavelength. It is shown that as  $L$  increases from 1 to 3, the achievable rate at high SNR increases. The rates converge to  $\log_2 K(4, L)$  bps/Hz, which is 4, 7 and 7.9 bps/Hz when  $L = 1, 2, 3$ , respectively. In addition, the rates only converge at very high SNR which is larger than 60 dB in the figure. The rates of the mmWave channel without quantization are also shown. We see that the loss incurred by the use of one-bit ADCs increases with the number of paths  $L$ .

### VII. CONCLUSION

In this paper, we analyzed the capacity of point-to-point  $N_t \times N_r$  MIMO channel with one-bit quantization at the receiver. CSI is assumed to be known at both the transmitter and receiver. We considered several specializations in our work. We derived the capacity of the MISO channel in closed-form. It was shown that MRT beamforming and QPSK signaling is the optimal transmission strategy. For the SIMO channel, we obtained the lower and upper bounds on the high SNR capacity. We found that the high SNR capacity of SIMO channel is close to the upper bound  $\log_2(4N_r + 1)$  when  $N_r$  is large. Through a numerical algorithm called cutting plane method, we found the optimal input distribution. For the MIMO channel, we derived the high SNR capacity by relating the problem to a classic combinatorial geometric problem. We proposed two heuristic methods to design the input alphabet: channel inversion and convex optimization. The first method achieves the high SNR capacity only when the channel is invertible. The second method can be applied to general MIMO channel but has higher complexity. Last, we

considered the mmWave MIMO channel with limited paths. We showed that multipath is helpful in improving the high SNR capacity. Finally, we proposed a transmission strategy to achieve the capacity when there is only one path in mmWave channel.

There are many potential directions of future work. Perhaps the most critical assumption is that the transmitter and receiver have complete and perfect CSI. The channel estimation with one-bit quantization has been considered in [26]–[30] at lower frequencies. In the mmWave channel, it is of interest to develop efficient compressed channel estimation techniques at the receiver and also methods for feeding back CSI to the transmitter. Initial work on channel estimation in the one-bit compressive sensing framework has been reported in [51], [52] and our work in [53].

### REFERENCES

- [1] J. Mo and R. Heath, "High SNR capacity of millimeter wave MIMO systems with one-bit quantization," in *Proc. of Information Theory and Applications (ITA) Workshop*, 2014.
- [2] T. Baykas, C.-S. Sum, Z. Lan, J. Wang, M. Rahman, H. Harada, and S. Kato, "IEEE 802.15.3c: the first IEEE wireless standard for data rates over 1 Gb/s," *IEEE Commun. Mag.*, vol. 49, no. 7, pp. 114–121, July 2011.
- [3] A. Ghosh, T. Thomas, M. Cudak, R. Ratasuk, P. Moorut, F. Vook, T. Rappaport, G. Maccartney, S. Sun, and S. Nie, "Millimeter-wave enhanced local area systems: A high-data-rate approach for future wireless networks," *IEEE J. Sel. Areas Commun.*, vol. 32, no. 6, pp. 1152–1163, June 2014.
- [4] T. Rappaport, S. Sun, R. Mayzus, H. Zhao, Y. Azar, K. Wang, G. Wong, J. Schulz, M. Samimi, and F. Gutierrez, "Millimeter wave mobile communications for 5G cellular: It will work!" *IEEE Access*, vol. 1, pp. 335–349, 2013.
- [5] W. Hong, K.-H. Baek, Y. Lee, Y. Kim, and S.-T. Ko, "Study and prototyping of practically large-scale mmWave antenna systems for 5G cellular devices," *IEEE Commun. Mag.*, vol. 52, no. 9, pp. 63–69, September 2014.
- [6] "Wilocity Chipsets." [Online]. Available: <http://wilocity.com/products/chipsets>
- [7] S. Rangan, T. Rappaport, and E. Erkip, "Millimeter-wave cellular wireless networks: Potentials and challenges," *Proc. IEEE*, vol. 102, no. 3, pp. 366–385, March 2014.
- [8] R. Walden, "Analog-to-digital converter survey and analysis," *IEEE J. Sel. Areas Commun.*, vol. 17, no. 4, pp. 539–550, 1999.
- [9] B. Murmann, "ADC performance survey 1997-2014." [Online]. Available: <http://www.stanford.edu/~murmann/adcsurvey.html>
- [10] B. Le, T. Rondeau, J. Reed, and C. Bostian, "Analog-to-digital converters," *IEEE Signal Process. Mag.*, vol. 22, no. 6, pp. 69–77, 2005.
- [11] "Texas instruments ADC products." [Online]. Available: <http://www.ti.com/lscds/ti/data-converters/analog-to-digital-converter-products.page>
- [12] S. Vitali, G. Cimatti, R. Rovatti, and G. Setti, "Adaptive time-interleaved ADC offset compensation by nonwhite data chopping," *IEEE Trans. Circuits Syst. II*, vol. 56, no. 11, pp. 820–824, 2009.
- [13] S. Ponnuru, M. Seo, U. Madhow, and M. Rodwell, "Joint mismatch and channel compensation for high-speed OFDM receivers with time-interleaved ADCs," *IEEE Trans. Commun.*, vol. 58, no. 8, pp. 2391–2401, 2010.
- [14] T. Sundstrom, B. Murmann, and C. Svensson, "Power dissipation bounds for high-speed Nyquist analog-to-digital converters," *IEEE Trans. Circuits Syst. I*, vol. 56, no. 3, pp. 509–518, 2009.
- [15] J. Singh, S. Ponnuru, and U. Madhow, "Multi-gigabit communication: the ADC bottleneck," in *IEEE International Conference on Ultra-Wideband*, 2009, pp. 22–27.
- [16] O. Dabeer, J. Singh, and U. Madhow, "On the limits of communication performance with one-bit analog-to-digital conversion," in *IEEE 7th Workshop on Signal Processing Advances in Wireless Communications*, 2006, pp. 1–5.
- [17] J. Singh, O. Dabeer, and U. Madhow, "On the limits of communication with low-precision analog-to-digital conversion at the receiver," *IEEE Trans. Commun.*, vol. 57, no. 12, pp. 3629–3639, 2009.

- [18] S. Krone and G. Fettweis, "Capacity of communications channels with 1-bit quantization and oversampling at the receiver," in *35th IEEE Sarnoff Symposium (SARNOFF)*, 2012, pp. 1–7.
- [19] G. Zeitler, A. Singer, and G. Kramer, "Low-precision A/D conversion for maximum information rate in channels with memory," *IEEE Trans. Commun.*, vol. 60, no. 9, pp. 2511–2521, 2012.
- [20] B. Murray and I. Collings, "AGC and quantization effects in a zero-forcing MIMO wireless system," in *IEEE 63rd Vehicular Technology Conference*, vol. 4, May 2006, pp. 1802–1806.
- [21] J. A. Nossek and M. T. Ivrlac̆, "Capacity and coding for quantized MIMO systems," in *Proceedings of the 2006 international conference on Wireless communications and mobile computing*, ser. IWCMC '06. New York, NY, USA: ACM, 2006, pp. 1387–1392.
- [22] M. Ivrlac̆ and J. Nossek, "Challenges in coding for quantized MIMO systems," in *IEEE International Symposium on Information Theory*, July 2006, pp. 2114–2118.
- [23] A. Mezghani and J. Nossek, "On ultra-wideband MIMO systems with 1-bit quantized outputs: Performance analysis and input optimization," in *IEEE International Symposium on Information Theory*, 2007, pp. 1286–1289.
- [24] —, "Analysis of Rayleigh-fading channels with 1-bit quantized output," in *IEEE International Symposium on Information Theory*, 2008, pp. 260–264.
- [25] —, "Analysis of 1-bit output noncoherent fading channels in the low SNR regime," in *IEEE International Symposium on Information Theory*, 2009, pp. 1080–1084.
- [26] O. Dabeer and U. Madhow, "Channel estimation with low-precision analog-to-digital conversion," in *IEEE International Conference on Communications (ICC)*, 2010, pp. 1–6.
- [27] G. Zeitler, G. Kramer, and A. Singer, "Bayesian parameter estimation using single-bit dithered quantization," *IEEE Trans. Signal Process.*, vol. 60, no. 6, pp. 2713–2726, 2012.
- [28] T. Lok and V.-W. Wei, "Channel estimation with quantized observations," in *IEEE International Symposium on Information Theory*, Aug 1998, p. 333.
- [29] M. T. Ivrlac̆ and J. A. Nossek, "On MIMO channel estimation with single-bit signal-quantization," in *ITG Smart Antenna Workshop*, 2007.
- [30] A. Mezghani, F. Antreich, and J. Nossek, "Multiple parameter estimation with quantized channel output," in *2010 International ITG Workshop on Smart Antennas (WSA)*, 2010, pp. 143–150.
- [31] A. Wadhwa and U. Madhow, "Blind phase/frequency synchronization with low-precision ADC: a Bayesian approach," in *Proc. of 51st Allerton Conference on Communication Control and Computing*, 2013.
- [32] A. Mezghani, M.-S. Khoufi, and J. Nossek, "Spatial MIMO decision feedback equalizer operating on quantized data," in *IEEE International Conference on Acoustics, Speech and Signal Processing, 2008. ICASSP 2008.*, 2008, pp. 2893–2896.
- [33] A. Mezghani and J. Nossek, "Belief propagation based MIMO detection operating on quantized channel output," in *IEEE International Symposium on Information Theory Proceedings (ISIT)*, 2010, 2010, pp. 2113–2117.
- [34] A. Mezghani, M. Rouatbi, and J. Nossek, "An iterative receiver for quantized MIMO systems," in *16th IEEE Mediterranean Electrotechnical Conference (MELECON)*, March 2012, pp. 1049–1052.
- [35] Z. Wang, H. Yin, W. Zhang, and G. Wei, "Monobit digital receivers for QPSK: Design, performance and impact of IQ imbalances," *IEEE Trans. Commun.*, vol. 61, no. 8, pp. 3292–3303, 2013.
- [36] H. Witsenhausen, "Some aspects of convexity useful in information theory," *IEEE Trans. Inf. Theory*, vol. 26, no. 3, pp. 265–271, May 1980.
- [37] J. Huang and S. Meyn, "Characterization and computation of optimal distributions for channel coding," *IEEE Trans. Inf. Theory*, vol. 51, no. 7, pp. 2336–2351, 2005.
- [38] R. O. Winder, "Single stage threshold logic," in *Proceedings of the Second Annual Symposium on Switching Circuit Theory and Logical Design*, Oct 1961, pp. 321–332.
- [39] J. G. Wendel, "A problem in geometric probability," *Math. Scand.*, vol. 11, pp. 109–111, 1962.
- [40] T. Cover, "Geometrical and statistical properties of systems of linear inequalities with applications in pattern recognition," *IEEE Transactions on Electronic Computers*, vol. EC-14, no. 3, pp. 326–334, June 1965.
- [41] L. Flatto, "A new proof of the transposition theorem," *Proceedings of the American Mathematical Society*, vol. 24, no. 1, pp. 29–31, 1970.
- [42] W. Hachem, P. Loubaton, J. Najim *et al.*, "Deterministic equivalents for certain functionals of large random matrices," *The Annals of Applied Probability*, vol. 17, no. 3, pp. 875–930, 2007.
- [43] A. M. Tulino and S. Verdú, "Random matrix theory and wireless communications," *Commun. Inf. Theory*, vol. 1, no. 1, pp. 1–182, Jun. 2004. [Online]. Available: <http://dx.doi.org/10.1516/0100000001>
- [44] S. P. Boyd and L. Vandenberghe, *Convex optimization*. Cambridge University Press, 2004.
- [45] L. L. Dines, "Systems of linear inequalities," *Annals of Mathematics*, vol. 20, no. 3, pp. 191–199, 1919. [Online]. Available: <http://www.jstor.org/stable/1967869>
- [46] R. Blahut, "Computation of channel capacity and rate-distortion functions," *IEEE Trans. Inf. Theory*, vol. 18, no. 4, pp. 460–473, 1972.
- [47] M. D. McDonnell, N. G. Stocks, C. E. M. Pearce, and D. Abbott, *Stochastic resonance: from suprathreshold stochastic resonance to stochastic signal quantization*. Cambridge University Press, 2008.
- [48] M. McDonnell, "Is electrical noise useful? [point of view]," *Proc. IEEE*, vol. 99, no. 2, pp. 242–246, 2011.
- [49] R. C. Daniels, R. W. Heath, T. S. Rappaport, and J. N. Murdock, *Millimeter Wave Wireless Communications*. Pearson Education, 2014.
- [50] C. A. Balanis, *Antenna theory: analysis and design*. John Wiley & Sons, 2012.
- [51] P. Boufounos and R. Baraniuk, "1-bit compressive sensing," in *42nd Annual Conference on Information Sciences and Systems*, March 2008, pp. 16–21.
- [52] L. Jacques, J. Laska, P. Boufounos, and R. Baraniuk, "Robust 1-bit compressive sensing via binary stable embeddings of sparse vectors," *IEEE Trans. Inf. Theory*, vol. 59, no. 4, pp. 2082–2102, April 2013.
- [53] J. Mo and R. Heath, "Channel estimation in millimeter wave MIMO systems with one-bit quantization," to appear in the *Asilomar Conference on Signals, Systems and Computers*, Nov. 2014.